Journal of Advanced Research 55 (2024) 131–144

Contents lists available at ScienceDirect

Journal of Advanced Research

journal homepage: www.elsevier.com/locate/jare

Original Article

Bavachinin protects the liver in NAFLD by promoting regeneration via targeting PCNA

Xi Dong [a,b,c,d], Shan Lu [e], Yu Tian [a,b,c,d], Han Ma [f], Yang Wang [a,b,c,d], Xuelian Zhang [a,b,c,d], Guibo Sun [a,b,c,d], Yun Luo [a,b,c,d,*], Xiaobo Sun [a,b,c,d,*]

[a] Institute of Medicinal Plant Development, Peking Union Medical College and Chinese Academy of Medical Sciences, Beijing 100193, China
[b] Beijing Key Laboratory of Innovative Drug Discovery of Traditional Chinese Medicine (Natural Medicine) and Translational Medicine, Beijing 100193, China
[c] Key Laboratory of Bioactive Substances and Resource Utilization of Chinese Herbal Medicine, Ministry of Education, Beijing 100193, China
[d] Key Laboratory of Efficacy Evaluation of Chinese Medicine Against Glyeolipid Metabolism Disorder Disease, State Administration of Traditional Chinese Medicine, Beijing 100193, China
[e] Beijing Increasepharm Safety and Efficacy Co., Ltd, Beijing, China
[f] School of Traditional Chinese Medicine, Capital Medical University, Beijing, China

HIGHLIGHTS

- Our current study reports an active compound, namely bavachinin (BVC), protects high fat diet-induced nonalcoholic fatty liver disease in golden hamsters.
- To identify the target of BVC, we introduce click chemistry-activity-based protein profiling (CC-ABPP) technology, which is a chemical proteomic approach that identifies potential targets interacting with probe-conjugated compounds.
- With the use of CC-ABPP, we identify proliferating cell nuclear antigen (PCNA) as the target of BVC. And validation experiments including Cellular thermal shift assay (CETSA), Drug affinity responsive target stability (DARTS), Surface-plasmon resonance (SPR) are carried out to verify the direct interaction between BVC and PCNA.
- With the use of molecular docking and co-immunoprecipitation, BVC is proved to bind to the pocket of PCNA, facilitating the interaction between PCNA and DNA polymerase delta,

GRAPHICAL ABSTRACT

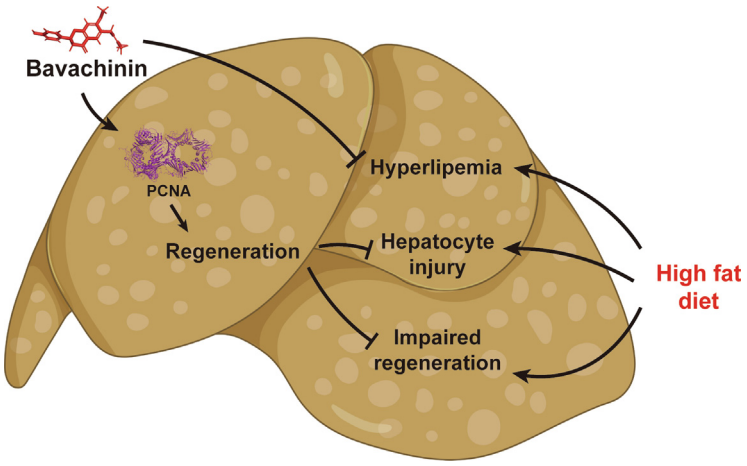

Abbreviations: ATO, atorvastatin; AOD, average optical density; BVC, bavachinin; BEC, biliary epithelial cell; CDE, choline-deficient ethionine-supplemented; CETSA, cellular thermal shift assay; CHO, cholesterol; CC-ABPP, click chemistry-activity-based protein profiling; Co-IP, co-immunoprecipitation; Pol δ, DNA polymerase δ; DARTS, drug affinity responsive target stability; DR, ductular reaction; H&E, hematoxylin and eosin; HFD, high fat diet; LC-MS/MS, Liquid Chromatography-Mass Spectrometry/Mass Spectrometry; LDL, low density lipoprotein; MFI, mean fluorescence intensity; NAFLD, nonalcoholic fatty liver disease; NASH, nonalcoholic steatohepatitis; OD, optical density; ORO, oil red O; PCNA, proliferating cell nuclear antigen; SPR, surface-plasmon resonance; TUNEL, terminal deoxynucleotidyl transferase-mediated dUTP nick-end labelling; TG, triglyceride.

Peer review under responsibility of Cairo University.

* Corresponding authors at: Institute of Medicinal Plant Development, Chinese Academy of Medical Sciences & Peking Union Medical College, No. 151 Malianwa North Road, Haidian District, Beijing, China.

E-mail addresses: ly20040423@126.com (Y. Luo), sun_xiaobo163@163.com (X. Sun).

https://doi.org/10.1016/j.jare.2023.02.007

while inhibits interaction between PCNA and p21. BVC's promotion on cell proliferation is then verified by CCK-8 staining, CFSE staining, and cell cycle assay.
- In NALFD golden hamsters, BVC protects hepatocytes and inhibits hepatocytes apoptosis, through promoting liver regeneration. Besides, BVC also ameliorates hyperlipemia.

ARTICLE INFO

Article history:
Received 1 September 2022
Revised 23 January 2023
Accepted 12 February 2023
Available online 16 February 2023

Keywords:
Bavachinin
CC-ABPP
NAFLD
Liver regeneration
PCNA

ABSTRACT

Introduction: Nonalcoholic fatty liver disease (NAFLD) is the most common liver disease all over the world, and no drug is approved for the treatment of NAFLD. Bavachinin (BVC) is proven to possess liver-protecting effect against NAFLD, but its mechanism is still blurry.
Objectives: With the use of Click Chemistry-Activity-Based Protein Profiling (CC-ABPP) technology, this study aims to identify the target of BVC, and investigate the mechanism by which BVC exerts its liver-protecting effect.
Methods: The high fat diet induced hamster NAFLD model is introduced to investigate BVC's lipid-lowering and liver-protecting effects. Then, a small molecular probe of BVC is designed and synthesized based on the CC-ABPP technology, and BVC's target is fished out. A series of experiments are performed to identify the target, including competitive inhibition assay, surface-plasmon resonance (SPR), cellular thermal shift assay (CETSA), drug affinity responsive target stability (DARTS) assay, and co-immunoprecipitation (Co-IP). Afterward, the pro-regeneration effects of BVC are validated *in vitro* and *in vivo* through flow cytometry, immunofluorescence, and the terminal deoxynucleotidyl transferase-mediated dUTP nick-end labeling (TUNEL).
Result: In the hamster NAFLD model, BVC shows lipid-lowing effect and improvement on the histology. PCNA is identified as the target of BVC with the method mentioned above, and BVC facilitates the interaction between PCNA and DNA polymerase delta. BVC promotes HepG2 cells proliferation which is inhibited by T2AA, an inhibitor suppresses the interaction between PCNA and DNA polymerase delta. In NAFLD hamsters, BVC enhances PCNA expression and liver regeneration, reduces hepatocyte apoptosis.
Conclusion: This study suggests that, besides the anti-lipemic effect, BVC binds to the pocket of PCNA facilitating its interaction with DNA polymerase delta and pro-regeneration effect, thereby exerts the protective effect against HFD induced liver injury.

Introduction

Nonalcoholic fatty liver disease (NAFLD) is the most common liver disease all over the world, which consists of different subtypes, ranging from simple steatosis to nonalcoholic steatohepatitis (NASH) [1,2]. Although simple steatosis in NAFLD might not lead to short-term morbidity or mortality, progression to NASH could result in fibrosis, liver failure, even hepatocellular carcinoma [1], and fibrosis progresses in 20 % of NAFLD patients [3]. To date, however, there is no approved drug for NAFLD by U.S. Food and Drug Administration or European Medicines Agency. So no specific therapy can be firmly recommended and any drug treatment would be off-label [4,5]. On the other hand, statins are suggested to improve cardiovascular outcome and to control hyperlipemia in patients with NAFLD [6,7]. Nevertheless, hepatotoxicity caused by statins remains a safety concern, and routine examination of liver function is warranted in patients with chronic liver disease to prevent possible liver injury [8–10].

The "two-hit" hypothesis is used to be a widely accepted mechanistic explanation to the pathophysiology of NAFLD [11]. However, the "multiple hit" hypothesis is now more prevalent because it provides precise explanation of NAFLD pathogenesis [12]. Such hits include insulin resistance, hormones, nutritional factors and so on. Because the liver possesses an extraordinary capacity of regeneration but frequently impeded in chronic liver disease, the impaired liver regeneration is therefore considered to be a kind of "hit" in NAFLD [13,14]. In NAFLD, NASH, and/or obese patients, steatosis is believed to be a risk factor for liver failure after hepatectomy, which hinders liver regeneration [15]. Enhance liver regeneration is beneficial to chronic liver disease including drug-induced liver injury [16,17], liver fibrosis [18,19], and so on. A recent study also emphasized pro-regenerative approach alleviated fibrosis in NASH model [20].

Table 1
Primers used for quantitative real-time PCR.

Gene	Primer sequence (5′ to 3′)	Species
GAPDH	F: TGAGATCCCACCAACATCAAAT R: CAGTAGAAGGTGTGGAGATGAT	Golden hamster
Ccnb1	F: ACCTGAACCTGAACCTGTTATGGA R: CACATCGCTCACGGCAAGAAT	Golden hamster
Ccnb2	F: TGAGGATGTCTCCATGAAGGAAGAG R: GCTGCCTGAGATACTGGTAGATGT	Golden hamster
Ppara	F: TGCTAAAGTACGGTGTGTATGA R: GAACTCCCTTGTGATGAAGCCA	Golden hamster
Cpt1a	F: GTTATCCACAAGCCAGACTCCTCAG R: ACACCATAGCCATCATCAGCAACC	Golden hamster
IL-6	F: GGACAATGACTATGTGTTGTTAGAA R: AGGCAAATTTCCCAATTGTATCCAG	Golden hamster
TNF-alpha	F: TGAGCCATCGTGCCAATG R: AGCCCGTCTGCTGGTATCAC	Golden hamster

Proliferating cell nuclear antigen (PCNA) is an annular homotrimer nuclear protein which surrounds DNA, and regulates DNA synthesis via interacting with proliferative or anti-proliferative molecular like DNA polymerase δ (Pol δ) or p21 in cell division [21,22]. In association with Pol δ, PCNA enhances its processivity thereby facilitating Pol δ function in DNA synthesis [22]. However, p21′s interaction with PCNA interferes PCNA-dependent Pol δ function [23]. PCNA is constantly used as a proliferative or regenerative marker because its exclusive expression in mitotic cells [24,25]. However, few study explorers PCNA's effect in liver regeneration and NAFLD besides a proliferative marker.

The activity-based protein profiling (ABPP) technology is a chemical proteomic approach that identifies potential targets interacting with probe-conjugated compounds [26,27]. And click chemistry (CC) strategy is introduced into the design of probes so that the functional state of target proteins in cells could be reflected [26]. Here, we report bavachinin (BVC), a natural compound from traditional Chinses medicine *Fructus Psoraleae*, ameliorates NAFLD in hamsters. In the meanwhile, BVC promotes liver regeneration *in vitro* and *in vivo*. Taking the advantage of CC-ABPP technology, PCNA is proven to be the target of BVC. These results suggest BVC ameliorates NAFLD by promoting liver regeneration via targeting PCNA.

Materials and methods

Ethics statement

The use of animals was approved by the Laboratory Animal Ethics Committee of the Institute of Medicinal Plant Development, Peking Union Medical College, and conformed to the Guide for the Care and Use of Laboratory (Approve no. SLXD-20190903001).

Experimental materials

BVC (≥98 % purity) is purchased from Chengdu Pufei De biotech company (Chengdu, China). Atorvastatin is obtained from Pfizer (NY, USA). The DMEM is purchased from HyClone (MA, USA). The CCK-8 solution is obtained from Solarbio (Beijing, China). The primary antibodies against F4/80, PCNA, Pol delta 3, p21 are obtained from Proteintech (Wuhan, China). The recombinant human PCNA protein and the primary antibody against Sox9 are obtained from Abcam (Cambridge, UK). The cell cycle and apoptosis analysis kit is purchased from Beyotime (Shanghai, China). The ROS dye is purchased from DOJINDO (KMJ, Japan). The fetal bovine serum, CFSE Cell proliferation kit, TRIZOL reagent, TUNEL assay kit, and co-immunoprecipitation kit are obtained from Thermo Fisher Scientific (MA, USA). The PrimeScript RT Reagent kit and SYBR Green is purchased from TAKARA (OSA, Japan).

Animals experiments, serum biochemical analysis, and histology

Male adult golden hamsters (100–120 g) are purchased from Beijing Vital River Laboratory Animal Technology Co., ltd. (Beijing, China). The hamsters are raised in controlled light conditions (12 h light/ 12 h dark). After 7 days' acclimation under standard laboratory conditions, the hamsters are randomly divided into five groups, namely, control (Ctrl), high fat diet (HFD), BVC 50 mg/kg, BVC 100 mg/kg, and atorvastatin (ATO) group. BVC and atorvastatin are suspended in 0.5 % (w/v) aqueous solution of TWEEN-20, and administrated by gavage for 4 weeks after 2 weeks' HFD treatment. Then, the hamsters are fasted overnight and sacrificed. The serum as well as the liver tissues are obtained and stored at −80 ℃. The liver tissues intended to perform morphological analysis are fixed in 4 % tissue fix solution. With the use of AU480 analyzer (Beckman Coulter, CA, USA), the serum from all groups are analyzed for biochemical indexes. Hematoxylin and eosin (H&E), Masson and oil red O staining are performed to analyze morphology and lipid deposition of the liver.

Cell culture

HepG2 cells are purchased from Guan Dao Biotechnology (Shanghai, China), and cultured in DMEM supplement with 10 % fetal bovine serum at 37 ℃ and 5 % CO_2. For the explorations of BVC and XQ's protections, as well as the best protective dose against palmitic acid (PA) treatment, 200 μM PA is incubated with HepG2 cells with or without series doses of BVC or XQ for 24-h. Then the viability of HepG2 cells are assessed using CCK-8 technology.

Cell viability assay

HepG2 cells are cultured in 96-well plate in condition described in the cell culture section. After treatment, the supernatant is discarded, and the CCK-8 work solution is added to incubate with cells. After 2 h of incubation, the OD values are determined using Synergy H1 microplate reader (BioTek, VT, USA), and viabilities are calculated.

Oxidative stress determination

HepG2 cells are cultured in 12-well plate in condition described in the cell culture section. After treatment, the supernatant is discarded, and HepG2 cells are digested and then incubated with ROS dye (DOJINDO, KMJ, Japan) for 30 min at 37 ℃. Cells are then analyzed by flow cytometry (BD FACSCalibur, NJ, USA).

Click chemistry activity-based protein profiling (CC-ABPP) assay

The protein concentration of cell lysate is examined utilizing the BCA protein assay and normalized to 5 mg/mL. Then, 400 μL cell lysate are incubated for 1 h with either XQ or DMSO at room temperature. The click reaction reagents are incorporated to the lysate and incubated for 1 h. Then, all samples are mixed with streptavidin beads and reacted for 2 h. The supernatant is obtained by centrifuging, and retained for western blot analysis or sliver staining before processing for LC-MS/MS.

Cellular thermal shift assay (CETSA)

The procedure of CETSA is in accordance with a previous study [28]. Briefly, 100 μL aliquots of HepG2 cell lysate is mixed with BVC, and the final concentration of BVC is 10 μM. In control group, cell lysate is incubated with DMSO, which is the solvent of BVC. The mixture is incubated at graded temperatures (37 ℃, 42 ℃, 47 ℃, 52 ℃, 57 ℃, 62 ℃, 67 ℃, 72 ℃) for 3 min. All mixtures are centrifuged for 15 min at 12000 rpm to obtained the supernatants. The supernatants are analyzed for the PCNA expression using SDS-PAGE.

Drug affinity responsive target stability (DARTS) assay

The procedure of DARTS is in accordance with a previous study [29]. Briefly, TNC buffer is added to 100 μL aliquots of HepG2 cell lysate. One aliquot is used as control group with no pronase or BVC added. 6 other aliquots are used as experimental groups, with graded concentration of BVC (0, 3.13, 6.25, 12.5, 25 and 50 μM) added. All groups are incubated for 1 h at room temperature, then pronase (0.3 μg/mL) is added to all experimental groups. After

incubation for another 30 min at room temperature, all samples are analyzed for the PCNA expression using SDS-PAGE.

Surface-plasmon resonance (SPR)

The Pioneer System was used for SPR analysis. The recombinant human PCNA protein is immobilized on the COOH5 Sensor Chip by 400 mM EDC/100 mM NHS-mediated crosslinking reaction. BVC and XQ are dissolved in 100 % DMSO to obtain a concentration of 5 mM and diluted in running buffer at concentrations ranging from 3.13 μM to 50 μM. The flow rate is 30 μL/min. The protein contact time was set to 60 s, and the disassociation time was set to 120 s. Data are analyzed using the Pioneer SPR System.

CFSE cell proliferation assay

The protocol of CFSE assay is in accordance with the reported study [30]. Briefly, cultured cells are digested and mixed gently to obtained single-cell suspension. After centrifuging for 5 min at 300g, cells are resuspend in PBS and supplement with 5 μM CFSE work solution. The staining is stopped by adding full medium. Cells are planted in the culture plate and underwent corresponding treatment. Flow cytometry (BD FACSCalibur, NJ, USA) are applied to analyze fluorescence intensity.

Cell cycle analysis

For the cultured cells, single-cell suspension is obtained by digestion and mixing gently. For the fresh liver, single-cell suspension of the liver cells is obtained by grind and filtration by 300 mesh. Then, pre-cooled 75 % alcohol is used to fix the single-cell suspension. After stored overnight at 4 ℃. The fixed suspension is stained using the cell cycle and apoptosis analysis kit abided by the instructions. All samples are then analyzed with the use of flow cytometry (BD FACSCalibur, NJ, USA).

Molecular docking

The crystal structure of PCNA (PDB ID, 1VYJ) is accessed from the Protein Data Bank, and the structure of BVC (PubChem CID 10337211) is accessed from the PubChem database. PCNA and BVC structures are prepared using AutoDockTools 1.5.6 (Molecular Graphics Laboratory, CA, USA). The docking parameters are set as previously described [31]. The optimal docking result is visualized using PyMOL software (The PyMOL Molecular Graphics System, Version 2.0 Schrödinger, LLC).

Co-Immunoprecipitation (Co-IP)

To analyze immunoprecipitation (IP), cells are lysed in IP buffer at 4 ℃ for 10 min. Then, the lysate is centrifuged for 10 min at 12000 rpm. The supernatant is absorbed, mixed with protein A agarose beads and the antibody, then incubated overnight at 4 ℃. The immunoprecipitated beads were then washed 3 times with Co-IP buffer, and the bound proteins are detected by western blot [32].

Western blots

The western blots are conducted according to previous study [26]. Briefly, 40 μg of total protein is loaded per lane, separated using 10 % SDS-PAGE, and blotted onto nitrocellulose membranes. The membranes are incubated overnight at 4 ℃ with primary antibodies allowing fully connections of antigens to antibodies. Then the membranes are washed with TBST, incubated with secondary antibodies. All bands are visualized using an ECL kit (CW0049, CWBIO, Beijing, China).

Immunofluorescence analysis

Paraffin embedded sections are dewaxed using graded ethanol. Then the sections are blocked with 5 % goat serum, incubated with primary antibodies overnight at 4 ℃. The secondary antibodies are incubated with the sections for one hour at room temperature. Then the images are acquired and analyzed by the TissueFAXS (Tissue Gnostics, CA, USA).

Immunohistochemistry analysis

The sections are treated according to the instruction of immunohistochemistry staining kit (ZSGB-BIO, Beijing, China). Briefly, paraffin embedded sections are dewaxed using graded ethanol and blocked with peroxidase inhibitors. Then all sections are incubated with primary antibody overnight at 4 ℃. The secondary antibody is incubated with the sections for one hour at 37 ℃. After labeled by DAB staining, the images are acquired by Aperio S2 Leica Biosystem microscopy (Leica, Wetzlar, Germany), and analyzed by Image-pro plus (Meyer Instruments, TX, USA).

Quantitative real-time polymerase chain reaction

The TRIZOL reagent is applied for the extraction of the total RNA from the frozen liver tissues. The extraction procedure abides by the manufacturer's instructions. Then, cDNA is synthesized from RNA using the PrimeScript RT Reagent kit, and analyzed by LightCycler 480 (Roche, Basel, Swiss). All primer pairs are provided in table 1.

Terminal deoxynucleotidyl transferase-mediated dUTP nick-end labeling assay

The terminal deoxynucleotidyl transferase-mediated dUTP nick-end labeling (TUNEL) assay is performed on the basis of instructions of the TUNEL kit. Briefly, liver sections are dewaxed, permeabilized and then TdT reaction and Click-iT reaction are performed. After the coloration by DAB reaction, liver sections images are acquired by Aperio S2 Leica Biosystem microscopy (Leica, Wetzlar, Germany). Image-pro plus (Meyer Instruments, TX, USA) is introduced to quantificat TUNEL positive cells.

Statistical analysis

Statistical Product and Service Solutions (IBM SPSS) software is used to test the normality and homogeneity of variance using the Kolmogorov-Smirnov and Levene's test. Data from two groups are compared using T tests on GraphPad Prism (GraphPad Software Inc., San Diego, CA). Data from three or more groups are compared using one-way ANOVA on GraphPad Prism (GraphPad Software Inc., San Diego, CA), using Dunnett's post hoc test to analyze the difference between groups. For those data that needs to be processed so that can be analyzed, data is performed by Z-score normalization then one-way ANOVA is used to compare different groups. The chi-square test is used to compare constituent ratio from different groups. Data are presented as mean ± SD or median with range. Differences are considered significant when the P value is <0.05.

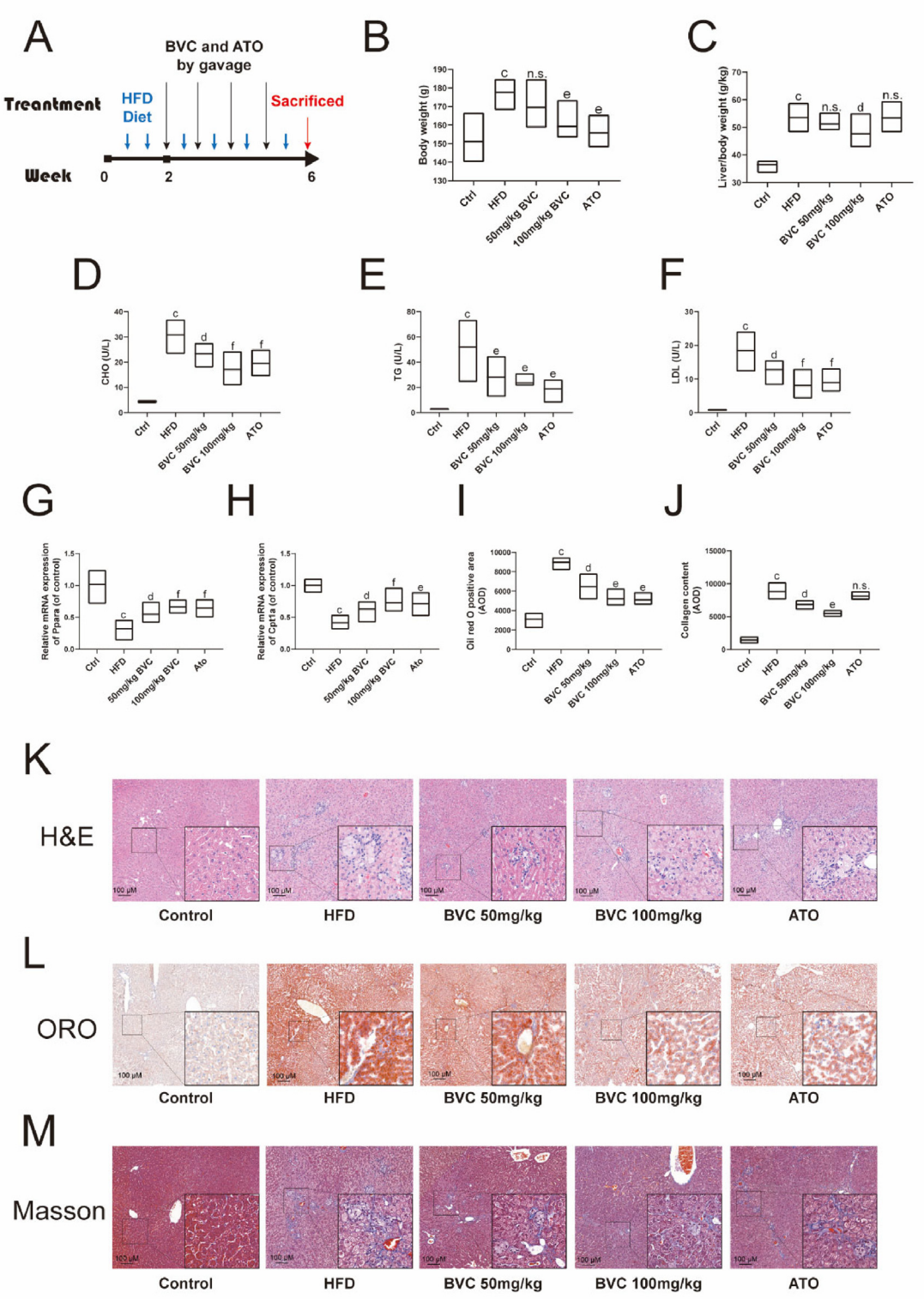

Fig. 1. BVC alleviates HFD induced NALFD. (A) Experimental design scheme. (B) BVC treatment decreases the body weight of the NAFLD hamster (n = 6). (C) BVC treatment reduces the liver to body weight of the NAFLD hamster (n = 6). (D-F) BVC treatment ameliorates serum CHO, TG, and LDL levels of NAFLD hamsters (n = 6). (G-H) BVC treatment elevates fatty acid oxidation related genes expression (n = 6). (I) BVC treatment decreases lipid deposition in NAFLD hamsters (n = 3). (J) BVC treatment decreases collagen content in NAFLD hamsters (n = 3). (K-M) Representative images of hematoxylin and eosin staining (K), oil red O staining (L), and Masson staining (M) of liver sections from NAFLD hamsters with BVC or atorvastatin treatments. All plots are presented as mean ± SD which are provided in Fig. S4. $^{a}P < 0.05$, $^{b}P < 0.01$, $^{c}P < 0.001$, n.s.† non-significant, compared with the control group; $^{d}P < 0.05$, $^{e}P < 0.01$, $^{f}P < 0.001$, n.s. non-significant, compared with the HFD group. (For interpretation of the references to colour in this figure legend, the reader is referred to the web version of this article.)

Results

Administration of BVC alleviates high fat diet-induced NAFLD in golden hamsters

The golden hamster has been used as a model exploring the treatments or pathologies of metabolic diseases such as NAFLD, because it shares similar lipid and lipoprotein metabolism pattern as that in humans [33]. The toxicity of BVC on the hamsters is firstly investigated. There is no obvious effect on the body weight after one-month administration BVC (2500 mg/kg/day to 161.25 mg/day) by gavage, same as its effects on the liver or heart to body weight ratio (supplement Fig. S1A-S1C). Although 2500 mg/kg BVC slightly increases the AST and CK-MB levels, they are still of no significance comparing with the control group just as LDH level (supplement Fig. S1D-S1F).

Then BVC's protective effects against high fat diet (HFD)-induced NAFLD are explored in the golden hamsters. To gain insights into the protective role of BVC in NAFLD, the hamsters are fed with HFD for 2 weeks and blood biochemical tests are performed to assure the hamsters get hyperlipemia (Fig. 1A and supplement Fig. S2). Then BVC is administered orally at 50 and 100 mg/kg/day to the HFD-induced NAFLD hamsters every day for 4 weeks, and 4 mg/kg atorvastatin is utilized as a positive control. Compared to the control group in which the hamsters are fed with normal chow, the body weight (Fig. 1B) and liver coefficient (liver to body weight ratio, Fig. 1C) of HFD group increases significantly. 100 mg/kg/day BVC is able to decrease the body weight and liver coefficient, while 50 mg/kg/day BVC has only slight effects on these indexes. On the other hand, atorvastatin is only capable of reducing body weight, but has no effect on liver coefficient. According to the blood biochemical tests, HFD elevates serum lipid (cholesterol, CHO; triglyceride, TG; Fig. 1D and 1E) and low density lipoprotein (LDL, Fig. 1F) levels significantly compared to the control group. BVC at different doses and atorvastatin are all able to decrease serum lipid levels and LDL level. Additionally, fatty acid oxidation-related genes including *Ppara* and *Cpt1a* are significantly decreased by HFD feeding. Both doses of BVC and atorvastatin all increase their expressions dramatically (Fig. 1G and 1H).

Next, the liver histology is examined. The result of hematoxylin and eosin (H&E) staining indicates existence of the liver injury as well as the lymphocytes infiltration in the HFD group (Fig. 1K). 50 and 100 mg/kg BVC alleviate HFD induced liver injury, but the improvement on liver injury in the atorvastatin group is rather limited. The oil red O staining shows significant increase in the lipid deposition in HFD group, 50 and 100 mg/kg BVC could decrease lipid deposition, while 100 mg/kg BVC possesses better effect (Fig. 1I and 1L). The atorvastatin's effect is similar to the 100 mg/kg BVC group. Likewise, Masson's staining demonstrates alleviated fibrosis in the liver treated by BVC, while atorvastatin does not have positive effect on the fibrosis (Fig. 1J and 1 M).

Administration of BVC alleviates inflammation in NAFLD

Macrophages contribute to the initiation and progression of NAFLD through eliciting liver inflammation and hepatic damage [34]. We therefore detecting the levels of IL-6 and TNF-α which are secreted by macrophages [35], as well as the expression of F4/80, a marker of macrophages. Our results indicate HFD feeding increases IL-6 and TNF-α genes expression, while 50 and 100 mg/kg BVC all decrease their expressions. Although atorvastatin also slightly decreases IL-6 and TNF-α genes expression, it fails to reach statistical significance (Fig. 2A and 2B). The expression of F4/80 in the liver suggests the similar result (Fig. 2C and 2D). Both doses of BVC decrease F4/80 expression, but atorvastatin does not decrease it significantly. Those results suggest BVC treatments alleviates inflammation in NAFLD.

The synthesis of BVC probe and target profiling by BVC probe

The BVC probe (XQ) is synthesized to identify the target of BVC, and the scheme of synthesis process is displayed in Fig. 3A. Afterward, we compare the anti-lipotoxicity effect of XQ with BVC to assure they have similar biological activity. The result indicates XQ possesses comparable anti-lipotoxicity effect as BVC in palmitic

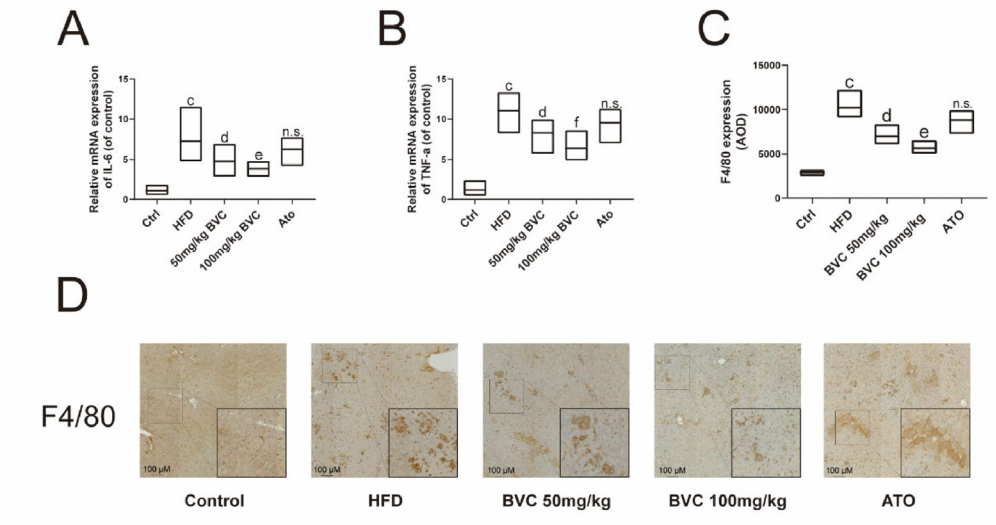

Fig. 2. BVC alleviates HFD induced inflammation. (A-B) BVC treatment decreases IL-6 and TNF-alpha genes expressions in the livers of NAFLD hamster (n = 6). (C) BVC treatment decreases F4/80 expression in the livers of NAFLD hamster (n = 3). (D) Representative images of F4/80 staining of the NAFLD hamster liver. All plots are presented as mean ± SD which are provided in Fig. S4. $^{a}P < 0.05$, $^{b}P < 0.01$, $^{c}P < 0.001$, n.s.† non-significant, compared with the control group; $^{d}P < 0.05$, $^{e}P < 0.01$, $^{f}P < 0.001$, n.s. non-significant, compared with the HFD group.

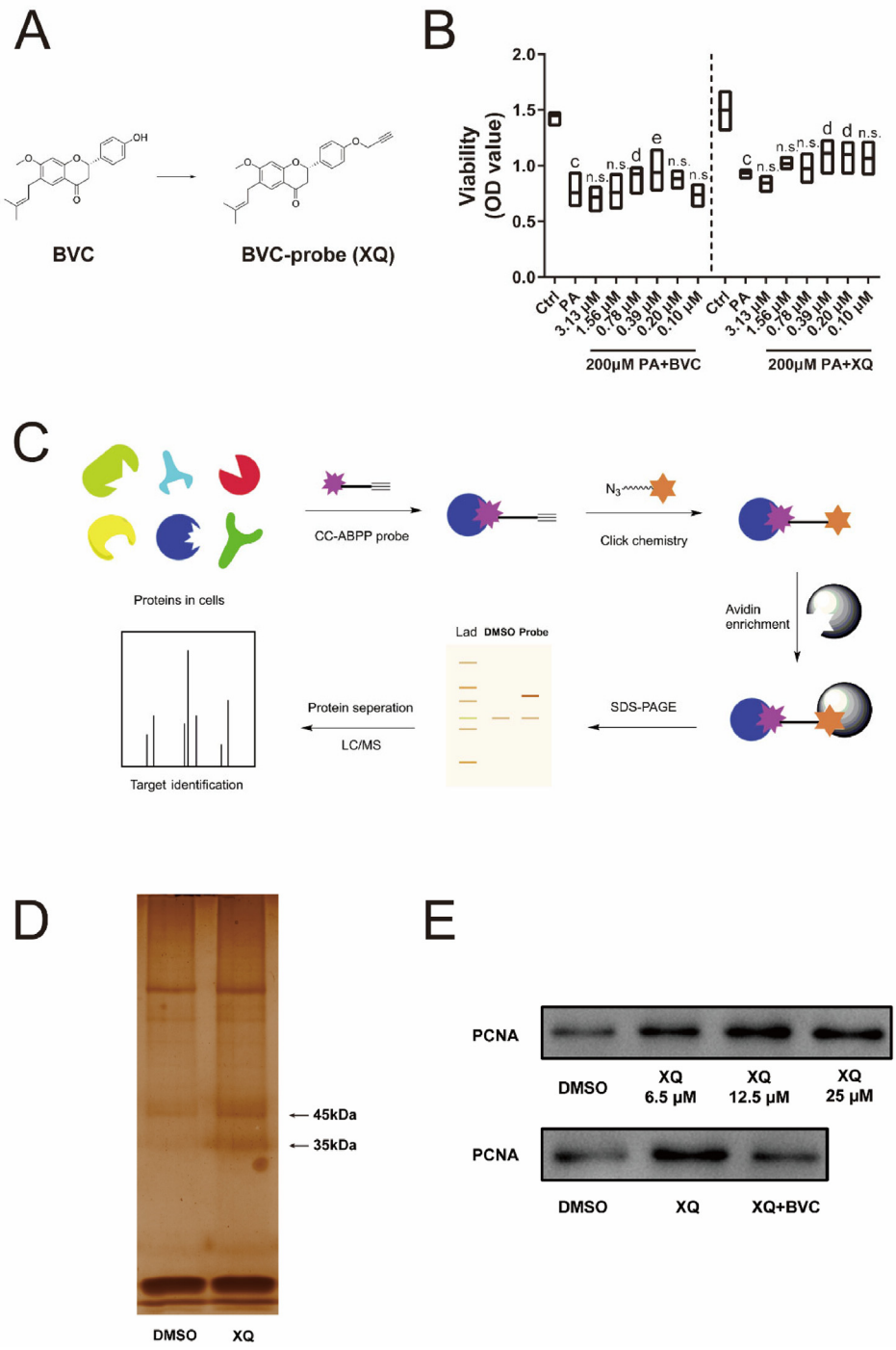

Fig. 3. CC-ABPP identified PCNA as a target of BVC. (A) Synthesis of biotinylated probe XQ. (B) XQ and BVC share similar protective effect on palmitic acid induced cytotoxicity. (C) Schematic diagram depicting target-fishing by XQ in cell lysate. (D) Silver stained proteins co-precipitated with XQ. (E, *Up*) The target-fishing of PCNA by XQ is in a dose-dependent manner. (E, *Down*) BVC competitively inhibited the binding of XQ to PCNA. All plots are presented as mean ± SD which are provided in Fig. S4. $^{a}P < 0.05$, $^{b}P < 0.01$, $^{c}P < 0.001$, n.s.† non-significant, compared with the control group; $^{d}P < 0.05$, $^{e}P < 0.01$, $^{f}P < 0.001$, n.s. non-significant, compared with the PA group.

acid-injured cell model and can be applied for target fishing (Fig. 3B). Oxidative stress is an important aspect of lipotoxicity, and is involved in the pathophysiology of NAFLD [36]. We therefore verify BVC's effects on the production of ROS. As is shown in supplement Fig. S3A and S3B, ROS level in HepG2 cells is significantly elevated by PA treatment, which is decreased by BVC treatments. The protein targets interacting directly with XQ are then identified in proteomes [27]. Briefly, XQ is completely incubated with HepG2 cell protein lysate to conduct the click chemical reaction, same amount of DMSO is used as control. Proteins bound to XQ are captured by streptavidin beads from protein lysate (Fig. 3C). The proteome is then eluted from the beads, separated by electrophoresis. As is shown in Fig. 3D, there are 2 obvious bands between 35 and 45 kDa in the XQ lane, but fading in the DMSO lane. The results suggest proteins in those bands are pulled by XQ and probably the target protein of BVC. So the bands are isolated, enzymatically hydrolyzed, and then subjected to LC-MS/MS identification. The identified peptide sequences are then matched

with the database, and all the results are supplied in Supplemental Data. We screen the data using a strict cut-off fold change of 2 and score $\geq$ 5 to serve as a criterion [26], and the proliferation cell nuclear antigen (PCNA, 36 kDa) gets a relatively high score and is closely related to regeneration, which is an intrinsic and unique feature of the liver in mammal. The mammalian liver protects itself against the internal and external insults by means of regeneration. Enhancing regeneration is also a therapeutic method for chronic liver disease [37]. Therefore, PCNA might be the target of BVC against NAFLD.

The affinity of different concentrations of XQ to PCNA is then analyzed. The result indicates affinity between them is in a dose-dependent manner, where 12.5 μM XQ possesses the strongest interaction with PCNA (Fig. 3E). To verify whether the structure modification affects the binding characteristics of BVC, we perform competitive inhibition experiment by capturing PCNA from cell lysate with XQ, or XQ plus BVC. BVC competes with XQ on the capture of PCNA, suggesting they share the same binding characteristics to PCNA. Therefore, the structure modification should not alter the binding property of XQ, at least not when binding to PCNA.

BVC interacts directly with PCNA and promotes the proliferation of HepG2 cells

Thereafter, a variety of validation experiments are carried out to verify the interaction between BVC and PCNA. The cellular thermal shift assay (CETSA) is a technology that evaluates drug-binding to the target protein based on the biophysical principle that thermal stabilization of target protein enhances after binding to the ligand [38]. As is shown in Fig. 4A, BVC significantly improves the thermal stabilization of PCNA at 57 ℃ and 62 ℃ comparing with the DMSO group. Drug affinity responsive target stability (DARTS) assay is also a technology confirming ligand-target binding which relies on decreased protease susceptibility of the target protein after binding to the ligand [39]. Our result indicates BVC stabilizes PCNA in cell lysate after treating with pronase [26], and the strongest effect is occurred at 6.25 μM (Fig. 4B). Surface plasmon resonance (SPR) is an optical technique used to measure molecular interactions in real time. SPR detects the changes of refractive index in the vicinity of thin metal layers reflecting biomolecular interactions [40]. The SPR result indicates BVC binds to PCNA in a dose-dependent manner, and the K_D value is 2.8 μM (Fig. 4C). These results all suggest BVC binds directly to PCNA.

Because PCNA has a key role in the DNA synthesis [22], we investigate the effects of BVC on the proliferation of HepG2 cells. The result indicates 6.25 and 3.13 μM BVC have toxic effect, while 0.2 and 0.1 μM BVC exhibit obvious proliferative effect on HepG2 cells after 24 h treatment (Fig. 4D), so we further explore their effects on cell growth with CFSE staining experiment, and we use 5 % FBS medium as a positive control. In the CFSE staining experiment, reduced fluorescence intensity represents cell proliferation [30]. As is shown in Fig. 4E and 4F, the BVC groups are of no significance when comparing with the control group in 24 h, but 5 % FBS has begun to exhibit obvious proliferative effect. After 48 h or 72 h of treatment, however, BVC at different doses all display significant proliferative effects, which is though less strong than 5 % FBS. Interestingly, we notice a phenomenon that HepG2 cells are treated with BVCs for 24 h when we identify the best action dose of BVC. On the other hand, the results from CFSE staining experiment demonstrate that 48 h BVC treatment begins to display positive effect. We speculate the inconformity might come from sensibility variances in different assays.

To verify this assumption, we conduct cell cycle assay, a sensitive approach that detects DNA mass in cells and thereby determines phases of cell cycle [19]. The results indicate both 0.2 and 0.1 μM BVC treatment decrease G0/G1 and S phases after 8 h treatment significantly. In the meanwhile, BVC treatments increase G2/M phases significantly. On the other hand, 5 % FBS sharply increases S and G2/M phases (Fig. 4G and 4H). After 16 h treatment, BVCs and 5 % FBS all decrease S phase, and increase G2/M phase. Besides, after 8 h culture, the constituent ratios of G0/G1 and S phases are around 40 % in all groups, while G2/M phases are around 20 %. After 16 h treatment, however, the constituent ratio of G0/G1 elevates sharply to around 70 %, and S phase drops to around 20 %, G2/M to 10 % in all groups, respectively (Fig. 4I and 4 J). These results suggest the proliferative effect of BVC initializes no later than 8 h in the terms of DNA synthesis and cell cycle progression. And after 16 h culture, cells are tended to slow down their growth.

BVC facilitates the interaction of PCNA with polymerase δ

After we confirm BVC's direct interaction with PCNA and its proliferative effects, we begin to wonder at what site does BVC bind to PCNA. PCNA has several binding sites for different ligand, including Pol δ, p21, pol ε, cyclin D and so on [41]. To predict the binding site and pattern of BVC to PCNA [42], we try to construct a model of BVC-PCNA complex taking advantage of AutoDockTools (ADT) software. We use ADT to calculate the binding energy of BVC to different binding sites, and the best result is obtained at the pocket for Pol δ and p21 binding (Fig. 5A) [41], suggesting BVC fits favorably to this pocket. And the constructed model predicted BVC has a contact with ASP-10 of PCNA. Besides, the different cell cycle distribution pattern induced by BVC might also suggest its interaction with Pol δ and p21′s pocket. As we mentioned above, BVC decreases S phase ratio and increases G2/M ratio throughout 16 h treatment, indicating its stable and persistent effects in cell cycle regulation. PCNA facilitates DNA synthesis in S phase by interaction with Pol δ [32]. On the other hand, p21′s interaction with PCNA results in reluctant progression through S phase [21,43]. BVC's promotion on S to G2/M progression might be ascribed to the enhancement of PCNA-Pol δ interaction and inhibition of PCNA-p21 interaction.

Next, we conduct the Co-IP experiment to explore the effect of BVCs at different concentrations on the binding of Pol δ or p21 to PCNA. As is shown in Fig. 5B, BVCs influence the binding of Pol δ/p21to PCNA in a dose-dependent manner. 2 μM BVC can sharply enhance the binding of PCNA to Pol δ. In the meantime, p21′s binding to PCNA is dramatically reduced by 2 μM BVC. 10, 50 μM BVC weaken their influence on the Pol δ/p21-PCNA binding gradually. The Pol δ and p21 compete on the binding to the same pocket on PCNA thereby facilitating or suppressing the proliferation-promoting effect of PCNA [44], our results indicate that BVC could bind to PCNA facilitating its interaction with Pol δ, while inhibiting the interaction with p21.

We next investigate whether the interference of the interaction between PCNA and Pol δ impacts BVC's proliferative function. T2AA is an inhibitor that binds to the PCNA at the cavity where Pol δ binds, thus interferes their interaction and cell proliferation [45]. This unique feature makes T2AA an ideal inhibitor to verify BVC's influences on the proliferation as well as PCNA-Pol δ interaction. To fully examine the effects of BVC, we also introduce LY294002, an PI3K inhibitor suppressing cell proliferation [46]. As is shown in Fig. 5C and 5D, BVC alone promotes HepG2 cells proliferation sufficiently as evidenced by dramatically reduced fluorescence intensity. T2AA or LY294002 significantly inhibits proliferation, but treatment with BVC cannot reverse it. BVC's incompetence in the rescue of T2AA implies competitive inhibition by T2AA. Although LY294002 possesses different mechanism in growth inhibition comparing with T2AA, its strong effect also incapacitates BVC for the rescue.

The cell cycle assay is also conducted to investigate influence of BVC plus with different inhibitors on cell cycle distribution. As is

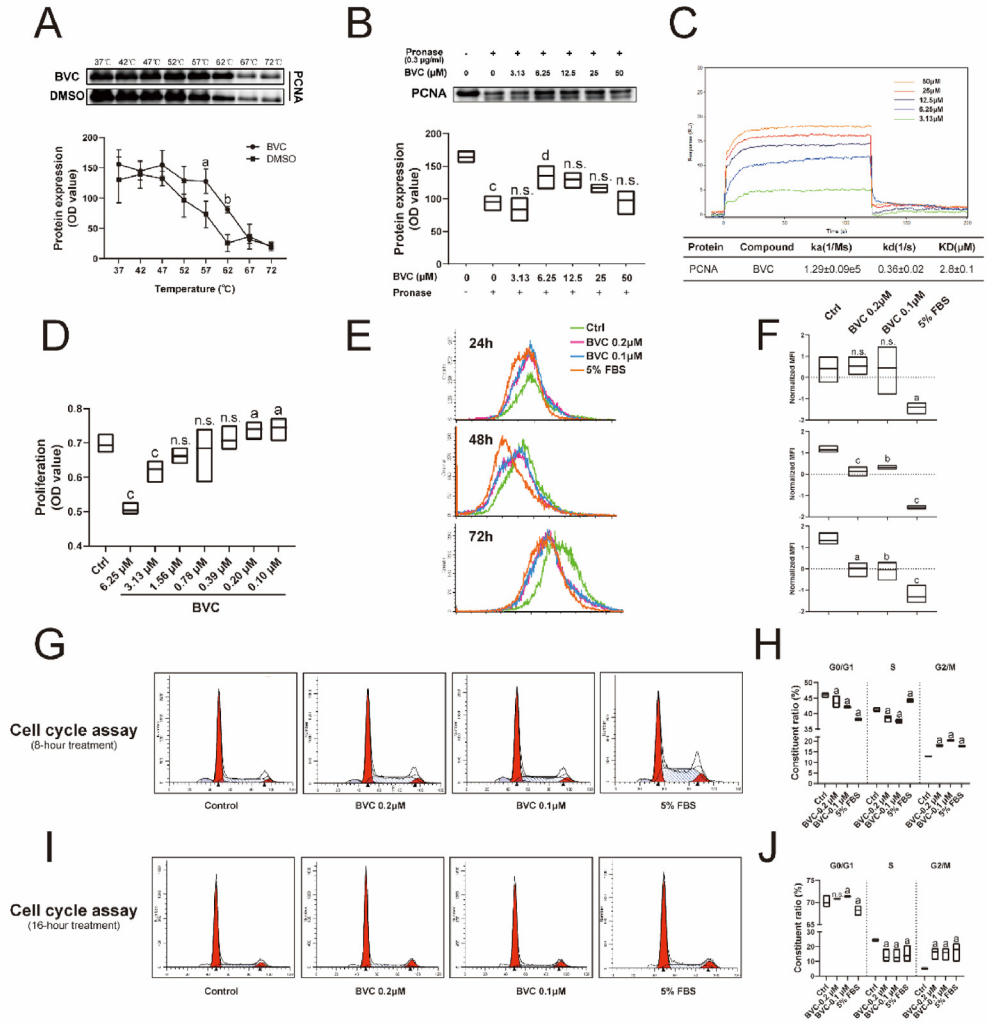

Fig. 4. Physiological validation of the BVC-PCNA interaction. (A) BVC treatment enhances the thermal stability of PCNA in cell lysates as determined by the CETSA (n = 3). (B) BVC treatment increases protease susceptibility of the PCNA in cell lysates as determined by the DARTS assay (n = 3). (C) BVC-PCNA interaction analysis based on SPR. (D) BVCs promote HepG2 cells proliferation (n = 3). (E) The overlay of the CFSE assay results demonstrating BVC treatments decrease CFSE fluorescence intensity (facilitates cell proliferation) of HepG2 cells. (F) Statistical analysis of CFSE assay, indicating BVC treatments for 48 h or 72 h exert significant proliferative effects (n = 3). (G) Representative images of cell cycle assay of 8 h BVC treatment on HepG2 cells. (H) Statistical analysis indicating 8 h BVC treatments promote the cell cycle entry of HepG2 cells (n = 3). (I) Representative images of cell cycle assay of 16 h BVC treatment on HepG2 cells. (J) Statistical analysis indicating 16 h BVC treatments promotes the cell cycle entry of HepG2 cells (n = 3). In the cell cycle assay, the differences between groups are determined by chi-square test using constituent ratio calculated on the basis of cell events from different phases. For better presentation, we show constituent ratio here but medians and ranges of original data in Fig. S4. All plots are presented as mean ± SD, or median with range which are provided in Fig. S4. $^{a}P < 0.05$, $^{b}P < 0.01$, $^{c}P < 0.001$, n.s.† non-significant, compared with the control group; $^{d}P < 0.05$, $^{e}P < 0.01$, $^{f}P < 0.001$, n.s. non-significant, compared with the model group (single-pronase treatment group).

shown in Fig. 5E and 5F, T2AA and LY294002 all have obvious impacts on cell cycle distribution, but are widely divergent in the distribution pattern. T2AA causes S and G2/M phases arrest, and reduce G0/G1 phase ratio. On the contrary, LY294002 shows no obvious effect on G0/G1 phase, but reduces S phase ratio while increases G2/M ratio. And G2/M ratio of LY294002 group is significantly higher than T2AA group (not labeled in Fig. 5F). T2AA and BVC have similar tendency to decrease G0/G1 and increase G2/M ratio comparing with the control group, but have opposite impacts on S phase ratio, which might be owing to their same binding sites on PCNA, but contrary effects. These data suggest BVC promotes HepG2 cells proliferation via interacting with PCNA.

Administration of BVC enhances liver regeneration in high fat diet-induced NAFLD golden hamsters

In chronic liver injury, liver regeneration is an intrinsic protective response against the insults, but always becomes insufficient due to unresponsive hepatocytes [47]. Because BVC exhibits obvious promotion on HepG2 cells proliferation, we therefore seek to uncover BVC's effect on the liver regeneration in NAFLD golden hamsters. The results show that G0/G1 phase of HFD group is significantly elevated while S and G2/M phases are reduced comparing to the control group, indicating insufficient regeneration against the lipotoxicity (Fig. 6A and 6B). 50 mg/kg BVC significantly increases S and G2/M phases proportion, and 100 mg/kg BVC slightly decreases S phase but sharply increases the G2/M phase proportion, suggesting BVC could enhance liver regeneration in the context of NAFLD. Atorvastatin, on the other hand, decreases G0/G1 phase proportion and increases S phase proportion, but has no obvious effect on the G2/M phase proportion.

To be fair, the cell cycle assay only depicts the distribution of different cycle phases, it can't distinguish proliferation from growth inhibition. So next, cell cycle genes expression are assessed. *Ccnb1* and *Ccnb2*, which are cyclin genes promoting cell cycle progression [19], are dramatically elevated in 100 mg/kg BVC group

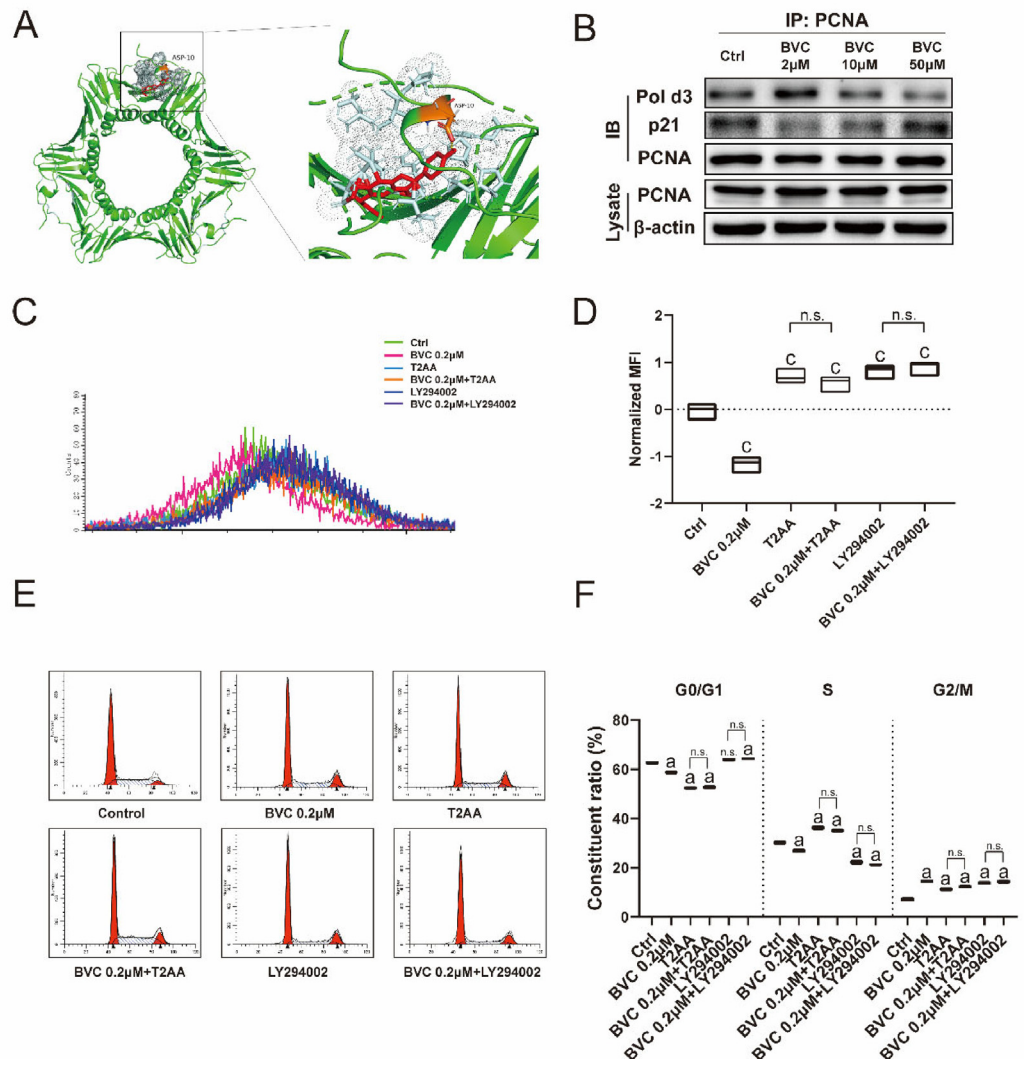

Fig. 5. Structural modeling and binding site validation of the BVC-PCNA interaction. (A, Left) Overview of BVC-PCNA complex model. PCNA is shown in cartoon representation in green, and BVC is shown in stick representation in red. The pocket of PCNA is shown in dot representation in gray. (A, Right) Zoom-in view of the predicted BVC-PCNA interface. BVC is predicted to have a H bond with ASP-10 of the PCNA. (B) Co-IP result indicating BVC facilitates the interaction between PCNA and Pol δ, while inhibits the interaction between PCNA and p21 (n = 3). (C) The overlay of the CFSE assay results. (D) Statistical analysis of CFSE assay, demonstrating T2AA and LY294002 treatments interfere BVC's proliferative effects on HepG2 cells (n = 3). (E) Representative images of cell cycle assay. (F) Statistical analysis indicating T2AA and LY294002 treatments interfere BVC's positive effects on cell cycle entry, but in different patterns (n = 3). In the cell cycle assay, the differences between groups are determined by chi-square test using constituent ratio calculated on the basis of cell events from different phases. For better presentation, we show constituent ratio here but medians and ranges of original data in Fig. S4. All plots are presented as mean ± SD, or median with range which are provided in Fig. S4. $^{a}P < 0.05$, $^{b}P < 0.01$, $^{c}P < 0.001$, n.s.† non-significant, compared with the control group. (For interpretation of the references to colour in this figure legend, the reader is referred to the web version of this article.)

comparing with the HFD group, suggesting enhanced regeneration in 100 mg/kg BVC group (Fig. 6C). Although *Ccnb1* and *Ccnb2* are all elevated in HFD, or 50 mg/kg BVC and atorvastatin groups, they are of no statistical significance when comparing to control group or HFD group, respectively. On the other hand, cycle inhibitor p21 (*Cdkn1a*) is increased in HFD, but inhibited by both doses of BVC. Beside, *Cdkn1a* is also slightly elevated in atorvastatin group.

Among various types of liver injury, there is a cell population that expresses biliary epithelial cell (BEC) marker such as Sox9, which is therefore termed reactive BECs. BECs expand from the periportal region to the surrounding parenchyma, and this phenomenon is known as the ductular reaction (DR). DR is correlated with liver regeneration and liver injury [48,49]. So we examine the PCNA and Sox9 expression in the liver of different groups. The PCNA expression of the HFD group, which represents the mitotic cells, is similar to that of the control group (Fig. 6D–6E). In the liver cell cycle assay, the proportions of S and G2/M phase of HFD group is decreased comparing with control group, suggesting the compromised regeneration. But PCNA expression indicates comparable regenerative ability between HFD and control groups. The difference between two results is probably due to the inconformity of different methodology as the cell cycle assay is based on the DNA content of the liver cells and therefore more sensitive. The 100 mg/kg BVC could increase PCNA expression significantly. But atorvastatin fails to up-regulate PCNA expression. So atorvastatin might also improve the regeneration of NAFLD to some degree, as evidenced by elevated S phase proportion. But this improvement is probably the by-product of anti-lipotoxicity, not due to the direct pro-regenerative effect. Because PCNA expression and *Cdkn1a* expression of the atorvastatin group stay statistically unchanged comparing to the control group. The expression of Sox9 is slightly elevated in the HFD group, indicating minorly enhanced DR (Fig. 6D and 6F). The inhibition of hepatocyte proliferation might be not serious, so the DR is only slightly enhanced.

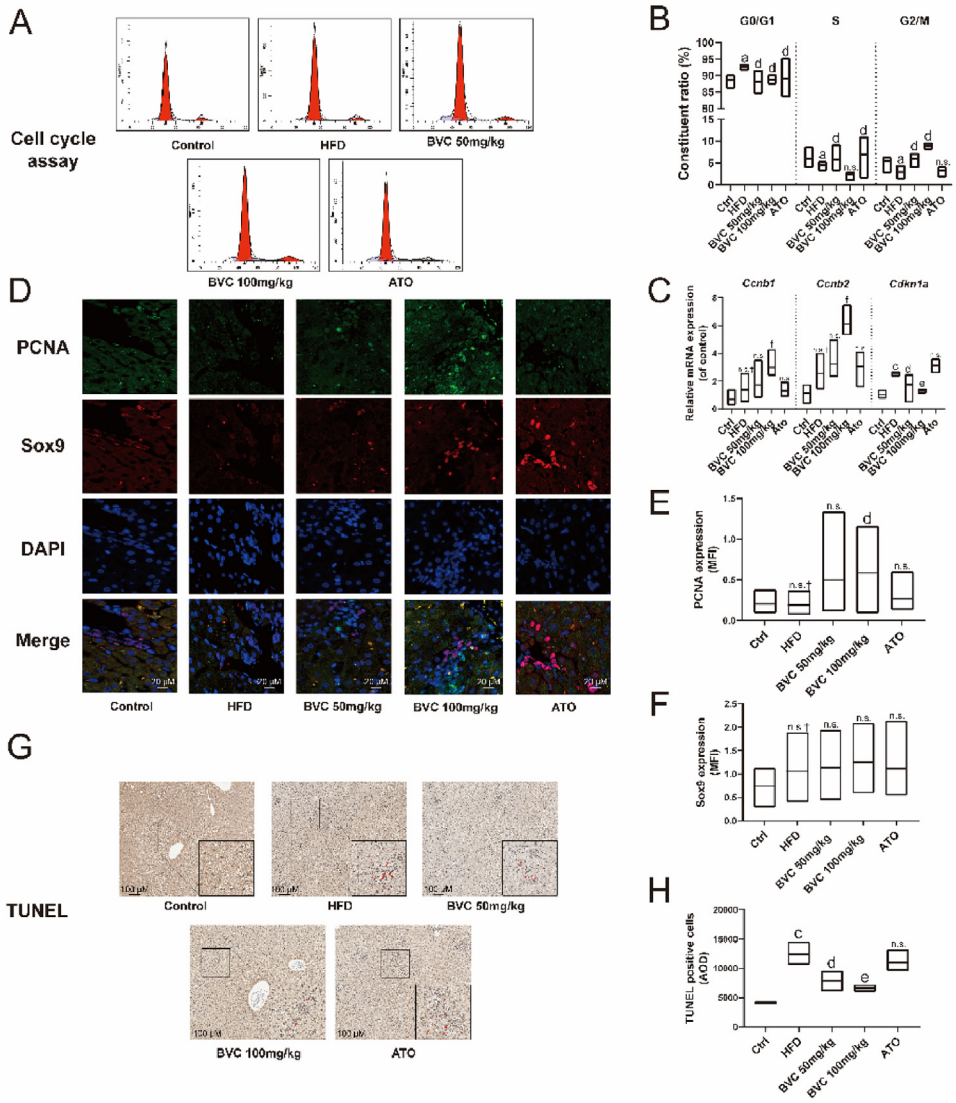

Fig. 6. BVC promotes liver regeneration and increases PNCA expression in NAFLD hamsters. (A) Representative images of cell cycle assay of liver cells from different groups of hamsters. (B) Statistical analysis indicating different doses of BVC exert various effects on S phase ratio, but all decrease G0/G1 phase ratio and increase G2/M phase ratio. Atorvastatin has no obvious effect on G2/M phase ratio (n = 6). (C) BVC treatments elevate cell cycle cyclin genes expressions and inhibit cell cycle inhibitor p21 expression, atorvastatin has no obvious effect on those genes (n = 6). (D) Immunofluorescence images of liver tissue sections from different groups of hamster stained with PCNA, Sox9, and DAPI (n = 3). (E-F) Statistical analysis of PCNA and Sox9 expressions in 6D. (G) Representative images of TUNEL assay from different groups of hamster's livers. (H) Statistical analysis indicates BVCs rescue liver cell apoptosis in hamsters, while atorvastatin fails to rescue (n = 3). In the cell cycle assay, the differences between groups are determined by chi-square test using constituent ratio calculated on the basis of cell events from different phases. For better presentation, we show constituent ratio here but medians and ranges of original data in Fig. S4. All plots are presented as mean ± SD, or median with range which are provided in Fig. S4. $^{a}P < 0.05$, $^{b}P < 0.01$, $^{c}P < 0.001$, n.s.† non-significant, compared with the control group; $^{d}P < 0.05$, $^{e}P < 0.01$, $^{f}P < 0.001$, n.s. non-significant, compared with the HFD group.

Analogously, the expressions of Sox9 in BVC and atorvastatin groups are similar to the HFD group.

Apoptosis is also a driven force to the regeneration. During tissue injury, the uninjured cells begin to proliferate so that the damaged cells are replaced, which is also termed "compensatory proliferation". During compensatory proliferation, the apoptosis cells generate mitogenic signals, and the uninjured cells begin to proliferate [50]. We therefore detect the apoptosis of liver cells. As are shown in Fig. 6G and 6H, TUNEL positive cells are significantly increased in HFD group, indicating the intensive apoptosis and liver injury. 50 and 100 mg/kg BVC are all exerting protective effects against HFD induced liver injury, while 100 mg/kg BVC possesses better effect. Atorvastatin does not exert obvious anti-apoptosis effect. These results imply BVC could enhance liver regeneration and thereby protecting liver in the NAFLD hamsters.

Discussion

To improve the histology or alleviate the progression of disease is the key point of the treatment to the NAFLD. However, there are no drugs for the treatment of NAFLD approved by U.S. Food and Drug Administration or European Medicines Agency. Drugs including statins, metformin, insulin and so on are recommended to control the metabolic syndrome, as NAFLD is frequently accompanied with obesity, hyperlipemia, or diabetes. However, there is no solid evidence that those drugs can benefit hepatocyte necrosis or inflammation [4]. In the present study, we show evidence that BVC is able to ameliorate the body weight and hyperlipemia in NAFLD hamster, and elevate the expressions of fatty acid oxidation related genes. In the meanwhile, histology and lipid deposition of the liver are also improved by the BVC treatment, which is consis-

tent with our previous study [51]. It is also worth to mention that, unlike atorvastatin, BVC improves the liver coefficient and histology in the hamsters, which suggests its protective role against NAFLD.

As discussed above, the lipid-control effect might not be closely associated with the liver protection in the context of NAFLD. Therefore, the ABPP technology is introduced to identify the target and to search the underlying liver-protecting mechanism of BVC. PCNA is thereafter identified as a direct target of BVC, which is an essential protein that is functionally involved in DNA replication, cell cycle progression, and so on [52]. Hence, PCNA is tightly linked to the intrinsic feature of mammalian liver—the regeneration. Unlike wound healing, regeneration is an inherent defense mechanism that produces new liver cells and thereby protects liver from chronic liver injuries including viral infections, alcohol and non alcoholic steatohepatitis (NASH), and so on [19,37]. Fibrosis, which is the by-product of the process of wound healing in all kinds of chronic liver injuries, is also inhibited by liver regeneration [53]. We suspect BVC's liver-protecting effect might come from its pro-regenerative function. Indeed, Enhanced regeneration is proved to alleviate the liver injuries in different animal models. In the bile duct ligation (BDL) or carbon tetrachloride (CCl_4) model, promoting liver regeneration is shown to resist liver fibrosis [37]. Furthermore, the transplantation of regenerative biliary epithelial cells (BECs) provides more direct evidence that promoting regeneration alleviates hepatic fibrosis and reduces mortality in biliary disease model [54]. A recent study also emphasizes that accelerated liver regeneration reduced HFD-induced hepatic steatosis [55]. Those studies all demonstrate the efficacy of regenerative treatment to the chronic liver injury.

Our results show that BVC facilitates the interaction between PCNA and Pol δ, while competitively inhibits the interaction of p21 with PCNA, thereby promoting cell proliferation *in vitro*. Next, the liver regeneration is evaluated in different groups of hamsters. Although the regeneration in NAFLD liver is sometime assessed after partial hepatectomy (PH) in animal model [56], hepatectomy is not a routine treatment to the NAFLD in clinical practice. We therefore evaluate the BVC's pro-regeneration effect against NAFLD without PH to mimic the clinical condition. Similar with the *in vitro* results, BVC exhibits pro-regenerative effect on the hamster liver, as is evidenced by the elevation of *Ccnb1* and *Ccnb2*, the decrease of *Cdkn1a*, and the promotion of cell cycle entry.

It is reasonable to concern about the rick of carcinogenesis after the BVC's proliferative effects are testified. Although cancer is characterized by uncontrolled proliferation, it is the result rather the reason of the cancer. Liver cancer usually comes from chronic liver injury of all kinds including virus infection, alcohol abuse, metabolic disorders and so on [57], where hepatocytes undergo continuous injury-repair cycle and eventually leads to tumorigenesis, or in other word, malignant proliferation. So it is the liver injury that precedes carcinogenesis, not the other way around. We prove that even 2500 mg/kg BVC administrated for one month does not alter the blood biochemistry (supplement Fig. S1), which suggest BVC is a rather safe compound. Besides, the liver to body weight ratio also stays unchanged after 2500 mg/kg BVC administration, suggesting that BVC does not possess the "proliferative effect" in the context of normal condition.

However, in the context of NAFLD where increased liver weight predicting structural changes [58], BVC alleviates the liver to body weight ratio, improves liver histology. This phenomenon implies BVC might possess the "pro-regenerative effect". Unlike malignant proliferation, regeneration occurs only when liver suffers from internal or external insults to generate new cells (not repair) and subsequently to reduce injuries. Regeneration is tightly controlled so that the carcinomatous change wouldn't happen. And extracellular matrix will not be produced in the process of regeneration [59]. Our Masson staining results also suggest BVC alleviates liver fibrosis. so there should be no risk of fibrosis or tumorigenesis.

To confirm the pro-regenerative effects of BVC, Sox9 and PCNA expressions is determined. Sox9 is a transcription factors that maintain the undifferentiated state of cells during organ development [60]. In the liver, Sox9 is expressed mainly in BECs. The expansion of the Sox9-positive BECs in the liver is termed the ductular reaction (DR), which exists and correlates with liver regeneration in almost all forms of liver injury [61]. However, hepatocyte proliferation is the principal mechanism for the liver regeneration, and DR only supplements when hepatocyte proliferation is inhibited. In the liver injury, the reactive BECs generate no more than 0.78 % of hepatocytes [62], while reaching 15.3 % even the liver p21 is overexpressed in the choline-deficient ethionine-supplemented (CDE) diet model [63]. Besides, DR exists in the liver specimen from non-alcoholic steatohepatitis (NASH) patients, and liver fibrosis at higher stages emerge higher grades of DR [64]. DR is therefore correlated with the progression of NAFLD where the hepatocytes are seriously inhibited, although DR's role in the liver injury is still controversial [65].

Our results demonstrate that BVC increases PCNA's expression in the NAFLD liver, which is consistent with the cell cycle-related gene expression and cell cycle assay, while atorvastatin has no obvious effect on it. Due to the limitation of our ssmethod suppology, we cannot stain mature hepatocyte marker like HNF4α to distinguish hepatocytes from BECs when PCNA and Sosx9 are co-stained. However, considering the massive amount of hepatocytes in the liver, and the finite contribution of BECs to the regeneration, it is reasonable to deduce enhanced PCNA expression exists mainly in the hepatocytes, in other words, hepatocytes proliferation accounts for the BVC's pro-regeneration effect. Besides, the location of PCNA positive cell also stands with this deduction (Fig. 6D).

We also notice that the Sox9 expression is elevated in HFD, BVC, and atorvastatin group, although there is no statistical significance among them. We infer that is because our NAFLD model is less advanced than NASH so the DR is not massively induced. Our results also suggest the improvements on the histology could not be attributed to the control of hyperlipemia, because atorvastatin displays a robust lipid-lowing effect but fails to ameliorate histology of the NAFLD liver. Hence, BVC's protection on the NAFLD probably relies on the promotion of hepatocyte regeneration, which stimulates liver's intrinsic feature to overcome the insults. The TUNEL assay is also in line with our analysis. BVC groups show decreased apoptosis, while atorvastatin doesn't when comparing with the HFD group. So our result suggests that, besides the antilipemic effect, BVC binds to the pocket of PCNA facilitating its interaction with Pol δ and pro-regeneration effect, thereby exerts the protective effects against HFD induced liver injury (Fig. 7).

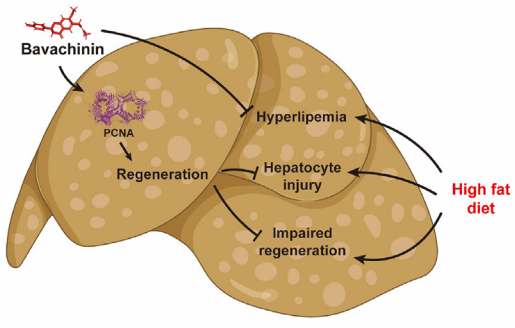

Fig. 7. Schematic diagram of the proposed mechanism of BVC action.

Conclusion

In summary, we confirm the anti-lipemic and liver-protecting effects of BVC, as evidenced by alleviation blood biochemical indexes, liver histology, apoptosis assay, and so on. With the use of CC-ABPP and LC-MS/MS technology, the PCNA is fished out and proven to be the target of BVC. Furthermore, the pro-regeneration effects of BVC is validated both *in vitro* and *in vivo*. We therefore deduce that BVC's liver-protecting effect against NAFLD is relied on its pro-regeneration effects.

Ethics statement:

The use of animals is approved by the Laboratory Animal Ethics Committee of the Institute of Medicinal Plant Development, Peking Union Medical College, and conformed to the Guide for the Care and Use of Laboratory (approve number: SLXD-20190903001).

CRediT authorship contribution statement

Xi Dong: Conceptualization, Methodology, Writing – original draft. **Shan Lu:** Software, Methodology. **Yu Tian:** Methodology. **Han Ma:** Software, Formal analysis. **Yang Wang:** Methodology, Data curation. **Xuelian Zhang:** Methodology. **Guibo Sun:** Validation. **Yun Luo:** Writing – review & editing, Visualization. **Xiaobo Sun:** Project administration, Funding acquisition.

Declaration of Competing Interest

The authors declare that they have no known competing financial interests or personal relationships that could have appeared to influence the work reported in this paper.

Acknowledgments

This article was supported by the CAMS Innovation Fund for Medical Sciences (CIFMS) (No. 2021-I2M-1-028), the National Natural Science Foundation of China (No. U20A20405). The authors would like to thank the AutoDockTools and PyMOL software for the molecular docking and result visualization.

Appendix A. Supplementary material

Supplementary data to this article can be found online at https://doi.org/10.1016/j.jare.2023.02.007.

References

[1] Review T, LaBrecque DR, Abbas Z, Anania F, Ferenci P, Khan AG, et al. World Gastroenterology Organisation global guidelines: nonalcoholic fatty liver disease and nonalcoholic steatohepatitis. J Clin Gastroenterol 2014;48:467–73.
[2] Wang FS, Fan JG, Zhang Z, Gao B, Wang HY. The global burden of liver disease: the major impact of China. Hepatology 2014;60:2099–108.
[3] Singh S, Allen AM, Wang Z, Prokop LJ, Murad MH, Loomba R. Fibrosis progression in nonalcoholic fatty liver vs nonalcoholic steatohepatitis: a systematic review and meta-analysis of paired-biopsy studies. Clin Gastroenterol Hepatol 2015;13(643–654).
[4] Cusi K, Isaacs S, Barb D, Basu R, Caprio S, Garvey WT, et al. American association of clinical endocrinology clinical practice guideline for the diagnosis and management of nonalcoholic fatty liver disease in primary care and endocrinology clinical settings: co-sponsored by the American association for the study of liver diseases [AASLD]. Endocr Pract 2022;28:528–62.
[5] L. European Association for the Study of the, D. European Association for the Study of, O. European Association for the Study of, EASL-EASD-EASO clinical practice guidelines for the management of non-alcoholic fatty liver disease. J Hepatol 2016;64:1388–402.
[6] Athyros VG, Tziomalos K, Gossios TD, Griva T, Anagnostis P, Kargiotis K, et al. Safety and efficacy of long-term statin treatment for cardiovascular events in patients with coronary heart disease and abnormal liver tests in the Greek Atorvastatin and Coronary Heart Disease Evaluation (GREACE) Study: a post-hoc analysis. Lancet 2010;376:1916–22.
[7] Ziaeian B, Dinkler J, Guo Y, Watson K. The 2013 ACC/AHA Cholesterol treatment guidelines: applicability to patients with diabetes. Curr Diab Rep 2016;16:13.
[8] Ward NC, Watts GF, Eckel RH. Statin toxicity. Circ Res 2019;124:328–50.
[9] Mancini GB, Baker S, Bergeron J, Fitchett D, Frohlich J, Genest J, et al. Diagnosis, prevention, and management of statin adverse effects and intolerance: Canadian consensus working group update [2016]. Can J Cardiol 2016;32: S35–65.
[10] Bjornsson ES. Hepatotoxicity of statins and other lipid-lowering agents. Liver Int 2017;37:173–8.
[11] Day CP. From fat to inflammation. Gastroenterology 2006;130:207–10.
[12] Buzzetti E, Pinzani M, Tsochatzis EA. The multiple-hit pathogenesis of non-alcoholic fatty liver disease (NAFLD). Metabolism 2016;65:1038–48.
[13] Jou J, Choi SS, Diehl AM. Mechanisms of disease progression in nonalcoholic fatty liver disease. Semin Liver Dis 2008;28:370–9.
[14] Dowman JK, Tomlinson JW, Newsome PN. Pathogenesis of non-alcoholic fatty liver disease. QJM 2010;103:71–83.
[15] Dutkowski P, Linecker M, DeOliveira ML, Mullhaupt B, Clavien PA. Challenges to liver transplantation and strategies to improve outcomes. Gastroenterology 2015;148:307–23.
[16] Dong J, Viswanathan S, Adami E, Schafer S, Kuthubudeen FF, Widjaja AA, et al. The pro-regenerative effects of hyperIL6 in drug-induced liver injury are unexpectedly due to competitive inhibition of IL11 signaling. Elife 2021;10.
[17] Shi L, Zhang S, Huang Z, Hu F, Zhang T, Wei M, et al. Baicalin promotes liver regeneration after acetaminophen-induced liver injury by inducing NLRP3 inflammasome activation. Free Radic Biol Med 2020;160:163–77.
[18] Ding BS, Nolan DJ, Butler JM, James D, Babazadeh AO, Rosenwaks Z, et al. Inductive angiocrine signals from sinusoidal endothelium are required for liver regeneration. Nature 2010;468:310–5.
[19] Dong X, Luo Y, Lu S, Ma H, Zhang W, Zhu Y, et al. Ursodesoxycholic acid alleviates liver fibrosis via proregeneration by activation of the ID1-WNT2/HGF signaling pathway. Clin Transl Med 2021;11:e296.
[20] Qing J, Ren Y, Zhang Y, Yan M, Zhang H, Wu D, et al. Dopamine receptor D2 antagonism normalizes profibrotic macrophage-endothelial crosstalk in non-alcoholic steatohepatitis. J Hepatol 2022;76:394–406.
[21] Cayrol C, Knibiehler M, Ducommun B. p21 binding to PCNA causes G1 and G2 cell cycle arrest in p53-deficient cells. Oncogene 1998;16:311–20.
[22] Mondol T, Stodola JL, Galletto R, Burgers PM. PCNA accelerates the nucleotide incorporation rate by DNA polymerase delta. Nucleic Acids Res 2019;47:1977–86.
[23] Huang Y, Zhu Y, Yang J, Pan Q, Zhao J, Song M, et al. CMTM6 inhibits tumor growth and reverses chemoresistance by preventing ubiquitination of p21 in hepatocellular carcinoma. Cell Death Dis 2022;13:251.
[24] Khamphaya T, Chukijrungroat N, Saengsirisuwan V, Mitchell-Richards KA, Robert ME, Mennone A, et al. Nonalcoholic fatty liver disease impairs expression of the type II inositol 1,4,5-trisphosphate receptor. Hepatology 2018;67:560–74.
[25] Xia J, Zhou Y, Ji H, Wang Y, Wu Q, Bao J, et al. Loss of histone deacetylases 1 and 2 in hepatocytes impairs murine liver regeneration through Ki67 depletion. Hepatology 2013;58:2089–98.
[26] Lu S, Tian Y, Luo Y, Xu X, Ge W, Sun G, et al. Iminostilbene, a novel small-molecule modulator of PKM2, suppresses macrophage inflammation in myocardial ischemia-reperfusion injury. J Adv Res 2021;29:83–94.
[27] Dai J, Liang K, Zhao S, Jia W, Liu Y, Wu H, et al. Chemoproteomics reveals baicalin activates hepatic CPT1 to ameliorate diet-induced obesity and hepatic steatosis. Proc Natl Acad Sci U S A 2018;115:E5896–905.
[28] Jafari R, Almqvist H, Axelsson H, Ignatushchenko M, Lundback T, Nordlund P, et al. The cellular thermal shift assay for evaluating drug target interactions in cells. Nat Protoc 2014;9:2100–22.
[29] Pai MY, Lomenick B, Hwang H, Schiestl R, McBride W, Loo JA, et al. Drug affinity responsive target stability (DARTS) for small-molecule target identification. Methods Mol Biol 2015;1263:287–98.
[30] Quah BJ, Warren HS, Parish CR. Monitoring lymphocyte proliferation in vitro and in vivo with the intracellular fluorescent dye carboxyfluorescein diacetate succinimidyl ester. Nat Protoc 2007;2:2049–56.
[31] Boittier ED, Tang YY, Buckley ME, Schuurs ZP, Richard DJ, Gandhi NS. Assessing molecular docking tools to guide targeted drug discovery of CD38 inhibitors. Int J Mol Sci 2020;21.
[32] Li G, Xie N, Yao Y, Zhang Y, Guo J, Feng Y, et al. Identification of PI3K regulatory subunit p55gamma as a novel inhibitor of vascular smooth muscle cell proliferation and neointimal formation. Cardiovasc Res 2015;105:75–85.
[33] Briand F, Maupoint J, Brousseau E, Breyner N, Bouchet M, Costard C, et al. Elafibranor improves diet-induced nonalcoholic steatohepatitis associated with heart failure with preserved ejection fraction in Golden Syrian hamsters. Metabolism 2021;117:154707.
[34] Schuster S, Cabrera D, Arrese M, Feldstein AE. Triggering and resolution of inflammation in NASH. Nat Rev Gastroenterol Hepatol 2018;15:349–64.
[35] Alciato F, Sainaghi PP, Sola D, Castello L, Avanzi GC. TNF-alpha, IL-6, and IL-1 expression is inhibited by GAS6 in monocytes/macrophages. J Leukoc Biol 2010;87:869–75.
[36] Masarone M, Rosato V, Dallio M, Gravina AG, Aglitti A, Loguercio C, et al. Role of oxidative stress in pathophysiology of nonalcoholic fatty liver disease. Oxid Med Cell Longev 2018;2018:9547613.
[37] Ding BS, Cao Z, Lis R, Nolan DJ, Guo P, Simons M, et al. Divergent angiocrine signals from vascular niche balance liver regeneration and fibrosis. Nature 2014;505:97–102.

[38] Martinez Molina D, Jafari R, Ignatushchenko M, Seki T, Larsson EA, Dan C, et al. Monitoring drug target engagement in cells and tissues using the cellular thermal shift assay. Science 2013;341:84–7.
[39] Lomenick B, Hao R, Jonai N, Chin RM, Aghajan M, Warburton S, et al. Target identification using drug affinity responsive target stability [DARTS]. Proc Natl Acad Sci U S A 2009;106:21984–9.
[40] Nguyen HH, Park J, Kang S, Kim M. Surface plasmon resonance: a versatile technique for biosensor applications. Sensors (Basel) 2015;15:10481–510.
[41] Maga G, Hubscher U. Proliferating cell nuclear antigen (PCNA): a dancer with many partners. J Cell Sci 2003;116:3051–60.
[42] Silakari O, Singh PK. Concepts and experimental protocols of modelling and informatics in drug design. 1. ed. Waltham: Elsevier; 2020.
[43] Waga S, Stillman B. Cyclin-dependent kinase inhibitor p21 modulates the DNA primer-template recognition complex. Mol Cell Biol 1998;18:4177–87.
[44] Waga S, Hannon GJ, Beach D, Stillman B. The p21 inhibitor of cyclin-dependent kinases controls DNA replication by interaction with PCNA. Nature 1994;369:574–8.
[45] Punchihewa C, Inoue A, Hishiki A, Fujikawa Y, Connelly M, Evison B, et al. Identification of small molecule proliferating cell nuclear antigen (PCNA) inhibitor that disrupts interactions with PIP-box proteins and inhibits DNA replication. J Biol Chem 2012;287:14289–300.
[46] Breslin EM, White PC, Shore AM, Clement M, Brennan P. LY294002 and rapamycin co-operate to inhibit T-cell proliferation. Br J Pharmacol 2005;144:791–800.
[47] Qian Y, Shang Z, Gao Y, Wu H, Kong X. Liver regeneration in chronic liver injuries: basic and clinical applications focusing on macrophages and natural killer cells. Cell Mol Gastroenterol Hepatol 2022.
[48] Roskams TA, Theise ND, Balabaud C, Bhagat G, Bhathal PS, Bioulac-Sage P, et al. Nomenclature of the finer branches of the biliary tree: canals, ductules, and ductular reactions in human livers. Hepatology 2004;39:1739–45.
[49] Ko S, Russell JO, Molina LM, Monga SP. Liver progenitors and adult cell plasticity in hepatic injury and repair: knowns and unknowns. Annu Rev Pathol 2020;15:23–50.
[50] Codispoti B, Makeeva I, Sied J, Benincasa C, Scacco S, Tatullo M. Should we reconsider the apoptosis as a strategic player in tissue regeneration? Int J Biol Sci 2019;15:2029–36.
[51] Dong X, Zhu Y, Wang S, Luo Y, Lu S, Nan F, et al. Bavachinin inhibits cholesterol synthesis enzyme FDFT1 expression via AKT/mTOR/SREBP-2 pathway. Int Immunopharmacol 2020;88:106865.
[52] Altieri AS, Ladner JE, Li Z, Robinson H, Sallman ZF, Marino JP, et al. A small protein inhibits proliferating cell nuclear antigen by breaking the DNA clamp. Nucleic Acids Res 2016;44:6232–41.
[53] Suarez-Cuenca JA, Chagoya de Sanchez V, Aranda-Fraustro A, Sanchez-Sevilla L, Martinez-Perez L, Hernandez-Munoz R. Partial hepatectomy-induced regeneration accelerates reversion of liver fibrosis involving participation of hepatic stellate cells. Exp Biol Med (Maywood) 2008;233:827–39.
[54] Hallett JM, Ferreira-Gonzalez S, Man TY, Kilpatrick AM, Esser H, Thirlwell K, et al. Human biliary epithelial cells from discarded donor livers rescue bile duct structure and function in a mouse model of biliary disease. Cell Stem Cell 2022;29:355–371 e310.
[55] Goikoetxea-Usandizaga N, Serrano-Macia M, Delgado TC, Simon J, Fernandez Ramos D, Barriales D, et al. Mitochondrial bioenergetics boost macrophage activation, promoting liver regeneration in metabolically compromised animals. Hepatology 2022;75:550–66.
[56] Valdecantos MP, Pardo V, Ruiz L, Castro-Sanchez L, Lanzon B, Fernandez-Millan E, et al. A novel glucagon-like peptide 1/glucagon receptor dual agonist improves steatohepatitis and liver regeneration in mice. Hepatology 2017;65:950–68.
[57] Bansal R, Nagorniewicz B, Prakash J. Clinical advancements in the targeted therapies against liver fibrosis. Mediators Inflamm 2016;2016:7629724.
[58] Sharawy MH, Abdel-Rahman N, Megahed N, El-Awady MS. Paclitaxel alleviates liver fibrosis induced by bile duct ligation in rats: Role of TGF-beta1, IL-10 and c-Myc. Life Sci 2018;211:245–51.
[59] Santos CC, Onofre-Nunes Z, Andrade ZA. Role of partial hepatectomy on Capillaria hepatica-induced hepatic fibrosis in rats. Rev Soc Bras Med Trop 2007;40:495–8.
[60] Kawaguchi Y. Sox9 and programming of liver and pancreatic progenitors. J Clin Invest 2013;123:1881–6.
[61] Machado MV, Michelotti GA, Pereira TA, Xie G, Premont R, Cortez-Pinto H, et al. Accumulation of duct cells with activated YAP parallels fibrosis progression in non-alcoholic fatty liver disease. J Hepatol 2015;63:962–70.
[62] Espanol-Suner R, Carpentier R, Van Hul N, Legry V, Achouri Y, Cordi S, et al. Liver progenitor cells yield functional hepatocytes in response to chronic liver injury in mice. Gastroenterology 2012;143:1564–1575 e1567.
[63] Raven A, Lu WY, Man TY, Ferreira-Gonzalez S, O'Duibhir E, Dwyer BJ, et al. Cholangiocytes act as facultative liver stem cells during impaired hepatocyte regeneration. Nature 2017;547:350–4.
[64] Gadd VL, Skoien R, Powell EE, Fagan KJ, Winterford C, Horsfall L, et al. The portal inflammatory infiltrate and ductular reaction in human nonalcoholic fatty liver disease. Hepatology 2014;59:1393–405.
[65] Williams MJ, Clouston AD, Forbes SJ. Links between hepatic fibrosis, ductular reaction, and progenitor cell expansion. Gastroenterology 2014;146:349–56.